Plasma Phys. Control. Fusion **51** (2009) 015015 (22pp) doi:10.1088/0741-3335/51/1/015015

Effect of electrostatic turbulence on magnetic islands

F L Waelbroeck[1], **F Militello**[1,2], **R Fitzpatrick**[1] **and W Horton**[1]

[1] Institute for Fusion Studies, The University of Texas, Austin, TX 78712-0262, USA
[2] EURATOM/UKAEA Fusion Association, Culham Science Centre, Abingdon, Oxfordshire, OX14 3DB, UK

Received 30 July 2008, in final form 27 October 2008
Published 11 December 2008
Online at stacks.iop.org/PPCF/51/015015

Abstract
A numerical analysis of the interaction of resistive drift wave and interchange turbulence with a magnetic island in a two-dimensional slab is presented. The time-scale for the evolution of the island is assumed to be much longer than that for the turbulence, allowing the use of an electrostatic model. The effects of the turbulence are isolated by choosing the parameters such that only even modes are unstable. This makes it possible to compare turbulent states with quiescent states in which turbulence is suppressed by enforcing odd parity. The turbulence is found to reduce the propagation velocity of the island. Its effect is destabilizing for thin islands but becomes stabilizing for islands greater than a few times the Larmor radius. Analysis of the quiescent solutions reveals the possibility of oscillations of the island amplitude and frequency through hysteretic transitions between bistable states.

(Some figures in this article are in colour only in the electronic version)

1. Introduction

The nonlinear phase of the tearing mode has been recognized for a long time as a fundamental plasma issue [1, 2]. In experimental fusion devices, the presence of magnetic islands associated with this mode can degrade the confinement and cause disruptions. A particular case observed in tokamaks is the neoclassical tearing mode (NTM) [3]. This mode is nonlinearly sustained by the perturbation of the pressure-gradient driven 'bootstrap' current. Its onset often limits the pressure in advanced tokamak configurations. The pressure gradient also drives short wavelength instabilities, however, such as drift waves and curvature-driven resistive interchange modes [4]. Island formation and evolution in tokamaks will thus occur in a turbulent environment. In stellarators, magnetic islands are sometimes created deliberately in the edge to serve as divertors. Such islands are likewise immersed in a turbulent bath [5]. The turbulent eddies and the magnetic island interact, thereby affecting the island amplitude and the relative rotation between the island and the surrounding plasma.

Early investigations of the effects of turbulence on linear tearing modes found that its primary effect is a diffusive broadening of the current channel [6]. A more recent investigation by Furuya *et al* used a one-point renormalization approach to model the effects of turbulence on a linear tearing mode in terms of anomalous dissipation coefficients [7]. McDevitt and Diamond subsequently examined the evolution of the drift-wave population density in the presence of a tearing mode using the wave-kinetic equation for an electrostatic model of the turbulence. They concluded that the turbulence gives rise to a negative viscosity that acts as a pump on the resonant long wavelength mode [8]. Ishizawa *et al* carried out numerical simulations of the evolution of the double-tearing mode in the presence of electromagnetic turbulence. They found that in a first stage, the zonal flows driven by the turbulence stabilize the linearly unstable double-tearing mode. In a second stage, however, long wavelength magnetic fluctuations exert a drag that suppresses the zonal flows, leading to the rapid growth of the double-tearing mode [9]. The effect of noise on NTM seeding has also been investigated by Itoh *et al* [10].

In this paper we analyze the mutual interaction between turbulent drift-wave fluctuations and a magnetic island. An earlier publication contains a brief description of the principal results of our research [11]. We focus on the regime where the width W of the island, defined as the distance across the O-point between the two branches of the separatrix, is of the order of the characteristic length scale of the turbulent eddies. The latter is typically a few times the ion Larmor radius calculated with the electron temperature, $\rho_s = c_s/\omega_{ci}$ where $c_s = \sqrt{T_e/m_i}$ is the cold-ion sound speed and ω_{ci} is the ion cyclotron frequency. We will express our results in terms of the normalized island width $w = W/\rho_s \sim 1$.

The work reported here forgoes the use of an electromagnetic model such as that used by Ishizawa [9] in favor of an electrostatic model. In an electrostatic model the island can be thought of as a perturbation of the magnetic field of fixed shape and amplitude. The island's rotation frequency ω, in contrast, evolves dynamically. The value of ω is determined by the vorticity equation and by the boundary conditions. The advantage of the electrostatic approximation is that it allows the island width to be set to any desired value without external forcing (which would affect the rotation frequency as well as the width of the island) and without the long simulation times needed for Ohmic relaxation. The electrostatic approximation facilitates the study of the dependence on the island width of various quantities and phenomena of interest such as the mode frequency, polarization current, background density flattening and turbulence.

The justification for the electrostatic approximation consists of two parts. For the short wavelength components (the turbulence), it requires that the magnetic fields generated by the turbulent polarization currents be negligibly small. This is the case whenever $\widehat{\beta} = \beta L_s^2/L_n^2 \ll 1$ (β is the ratio between the thermal and the magnetic pressure, L_s is the magnetic shear length and L_n the density scale length). For the long wavelength components (such as the magnetic island), in contrast, the electrostatic assumption requires that the reconnection rate be slow. This is the case when [12]

$$C(\Delta' + \Delta_{pol})\rho_s/\widehat{\beta}) \ll 1, \tag{1}$$

where $C = c^2\eta(8\pi)^{-1}\rho_s^{-2}\omega_*^{-1}\beta(L_s/L_n)^2$ is a measure of the plasma collisionality, Δ' is the standard linear stability parameter for the tearing mode [1, 13] and Δ_{pol} is the contribution of the internal polarization currents to the island evolution. Here η is the electrical resistivity, $\omega_* = v_* k_{y0}$ is the electron diamagnetic frequency, k_{y0} is the island poloidal wave number and $v_* = cT/(eB_z L_n)$ (e is the electric charge, T the constant electron temperature and c the speed of light). Note that C represents the skin time, normalized to the diamagnetic frequency, for a current sheet of width ρ_s. Equation (1) ensures a separation of scale between

the rate of change in the island width and the drift frequency characterizing the turbulent modes.

The paper is organized as follows: in section 2 we describe the derivation of the electrostatic model employed in our calculations, starting from an electromagnetic model. Section 3 sets forth the analysis of the linear stability of the system with respect to resistive drift waves and of its resulting tendency to spontaneously develop electrostatic turbulence. In section 4 we present and discuss the results of nonlinear numerical simulations of the interaction of drift waves with a magnetic island. Section 5 extends the preceding section by including the effect of the curvature of the magnetic lines, which induces interchange instabilities. Finally, in section 6 we summarize our results and draw conclusions.

2. Model

In order to clarify the approximations involved in the electrostatic model employed in our calculations, we show how to derive this model from an electromagnetic fluid model. We start from a simple model obtained from the standard two-fluid equations given in [14] by discarding the parallel momentum equation, neglecting the ion temperature terms, and reducing the dimensionality to two by restricting the perturbations to modes with the same pitch, or the same ratio of the toroidal to poloidal mode numbers. For simplicity, we also neglect the curvature terms except in section 5. We consider a 2D slab geometry periodic in y with a strong magnetic field B_z in the ignorable direction, $\boldsymbol{e}_z$. The magnetic field and the plasma $\boldsymbol{E}\times\boldsymbol{B}$ velocity take the form

$$\boldsymbol{B} = B_z\boldsymbol{e}_z + \boldsymbol{e}_z\times\nabla\psi, \tag{2}$$

$$\boldsymbol{v} = cB_z^{-1}\boldsymbol{e}_z\times\nabla\varphi, \tag{3}$$

where ψ is the magnetic flux and φ is the plasma stream function. The remaining equations describe the evolution of plasma vorticity, $U=\nabla^2\varphi$, the conservation of density, n, and the parallel component of Ohm's law:

$$\partial U/\partial t + \boldsymbol{v}\cdot\nabla U = \nabla_\parallel J + \mu\nabla^2 U, \tag{4}$$

$$\partial n/\partial t + \boldsymbol{v}\cdot\nabla n = \nabla_\parallel J + D\nabla^2 n, \tag{5}$$

$$\partial\psi/\partial t - \nabla_\parallel\varphi = -\nabla_\parallel n + CJ, \tag{6}$$

where $\nabla_\parallel F = \boldsymbol{B}\cdot\nabla F$ and J, defined by

$$J \equiv (1+\nabla^2\psi)/\widehat{\beta}, \tag{7}$$

is proportional to the perturbed plasma current along $\boldsymbol{e}_z$ (the normalization of J is chosen so as to eliminate factors of $\hat{\beta}$ from equations (4)–(5)). In system (4)–(6) the time is normalized with respect to the drift time, ω_*^{-1}, the transverse coordinates x and y are normalized to ρ_s and $L_y/2\pi$, respectively, where $2\pi\rho_s/L_y = K \ll 1$, the magnetic field is normalized to $\rho_s B'_{y0}$ where the prime denotes derivation with respect to x, the velocities to v_* and the density to a characteristic density n_0. The parameters D and μ are the normalized particle diffusion coefficient and the ion viscosity, respectively. We note that y represents the poloidal coordinate *in the island frame of reference*, and that in view of the normalization of y the azimuthal phase velocity and the frequency of the island are equal.

The above normalizations are such that all $\partial U/\partial t$ and $\partial n/\partial t$ in (4)–(5) are of order unity, so that $J\sim 1$ for $w\sim 1$. Integrating Ampere's law, equation (7), yields

$$\psi = -x^2/2 + \sum_m (\widetilde{\psi}_m(t) + \delta\widetilde{\psi}_m(x,t))\cos(my), \tag{8}$$

where $\delta\widetilde{\psi}_m \sim \hat{\beta}$. Thus, for $\hat{\beta} \ll 1$, the well-known constant-$\widetilde{\psi}$ approximation holds for all the modes (provided of course that the system is robustly stable to ideal MHD modes) [13]. The (un-normalized) Δ'_m stability parameter for tearing modes is negative for short wavelength modes, $\Delta'_m \sim -2k_y$, so that in general all but the longest wavelength mode are stable. Assuming this to be the case, the form of the flux simplifies to [1]

$$\psi = -x^2/2 + \widetilde{\psi}(t)\cos y, \tag{9}$$

where we drop the mode number index. We see that the magnetic field is completely determined once the island width, $w = 4\widetilde{\psi}^{1/2}$, is fixed. We note that equation (9) applies regardless of the sign of Δ'_1 and that despite the linear form of the flux perturbation, this equation allows the investigation of nonlinear effects when the island width exceeds the linear layer width.

The constant-$\widetilde{\psi}$ approximation makes it possible to replace Ohm's law by a scalar equation for the evolution of the island width. This scalar equation consists of the condition expressing the matching of the magnetic perturbation to its asymptotic form away from the island [13],

$$\frac{\Delta'\rho_s}{\widehat{\beta}} = \frac{1}{\widetilde{\psi}\pi}\int_{-l_x}^{l_x} \mathrm{d}x \int_{-\pi}^{\pi} \mathrm{d}y\, J\cos y, \tag{10}$$

where $\pm l_x$ denotes the boundaries of the slab and we have dropped the mode index on Δ'. Using Ohm's law to eliminate the current in (10) leads to

$$\frac{\mathrm{d}\widetilde{\psi}}{\mathrm{d}t} = \frac{C\Delta'\rho_s\widetilde{\psi}}{2l_x\widehat{\beta}} + \int_{-l_x}^{l_x}\frac{\mathrm{d}x}{2l_x}\int_{-\pi}^{\pi}\frac{\mathrm{d}y}{\pi}\cos y\,\nabla_\parallel(\varphi - n). \tag{11}$$

Note that in the second term on the right-hand side of equation (11), the integral attenuates the contribution of the short wavelength fluctuations. It follows that the magnitude of this term in turbulent conditions is comparable to that when the flow is laminar.

Equation (11) extends Rutherford's analysis [1] to cases where the island is out of equilibrium due to the turbulent fluctuations. In such cases the current varies along the field, $|\nabla_\parallel J| > 0$, so that J cannot be determined from the flux-surface average of Ohm's law as in [1]. Note that whenever equilibrium conditions do apply, the last term in equation (11) is proportional to $\mathrm{d}\widetilde{\psi}/\mathrm{d}t$ and combines with the similar term in the left-hand side of (11) in order to give Rutherford's well-known result.

Eliminating the current from the vorticity and continuity equations using Ohm's law yields

$$\frac{\partial U}{\partial t} + \boldsymbol{v}\cdot\nabla U = \frac{1}{C}\nabla_\parallel^2(n-\varphi) + \frac{x}{C}\frac{\mathrm{d}\widetilde{\psi}}{\mathrm{d}t}\sin y + \mu\nabla^2 U, \tag{12}$$

$$\frac{\partial n}{\partial t} + \boldsymbol{v}\cdot\nabla n = \frac{1}{C}\nabla_\parallel^2(n-\varphi) + \frac{x}{C}\frac{\mathrm{d}\widetilde{\psi}}{\mathrm{d}t}\sin y + D\nabla^2 n, \tag{13}$$

with boundary conditions described below. Equations (11)–(13) form a closed system for the fields φ, n, and the scalar amplitude $\widetilde{\psi}$. This system embodies the constant-$\widetilde{\psi}$ approximation and retains electromagnetic effects through equation (11).

For simplicity, we will reduce the problem further by restricting attention to islands close to saturation, such that $\mathrm{d}\widetilde{\psi}/\mathrm{d}t \approx 0$. That is, we assume that the two terms in (11) are in approximate balance. For such islands the equations reduce to

$$\frac{\partial U}{\partial t} + \boldsymbol{v}\cdot\nabla U = \frac{1}{C}\nabla_\parallel^2(n-\varphi) + \mu\nabla^2 U, \tag{14}$$

$$\frac{\partial n}{\partial t} + \boldsymbol{v}\cdot\nabla n = \frac{1}{C}\nabla_\parallel^2(n-\varphi) + D\nabla^2 n, \tag{15}$$

We denote the drive from the currents flowing in the vicinity of the island by the parameter Δ_{pol}:

$$\Delta_{\mathrm{pol}} \equiv \frac{\widehat{\beta}}{\rho_s C\widetilde{\psi}\pi}\int_{-l_x}^{l_x}\mathrm{d}x\int_{-\pi}^{\pi}\mathrm{d}y\,\nabla_\parallel(\varphi - n)\cos y, \tag{16}$$

This parameter measures the effect of the polarization currents on the evolution of the island. Calculating the change in $\Delta_{\rm pol}$ caused by the turbulence is one of the principal goals of this paper.

In order to complete system (14)–(15), we must supply boundary conditions for n, U and φ. For the density we impose $n(\pm l_x) = \mp l_x$, corresponding to a different density at each edge of the slab, fixed in time, so as to model the transport of particles down a density gradient. In order to motivate the choice of boundary conditions for U and φ, consider the azimuthal momentum conservation equation

$$(\partial_t + \boldsymbol{v}\cdot\nabla)\, v_y = -\partial_y n + J\widetilde{\psi}\sin y + \mu\nabla^2 v_y + \Gamma_y, \tag{17}$$

where $v_y = \partial_x\varphi$ is the azimuthal velocity and Γ_y denotes a source of momentum, such as a neutral-beam injector for example. Averaging the above equation over the simulation volume yields

$$\frac{\mathrm{d}\bar{v}_y}{\mathrm{d}t} = F_y + \Gamma_y + \mu[v_y']_{-l_x}^{l_x}. \tag{18}$$

Here,

$$\bar{v}_y \equiv \int_{-l_x}^{l_x}\frac{\mathrm{d}x}{2l_x}\int_{-\pi}^{\pi}\frac{\mathrm{d}y}{2\pi}\, v_y = \int_{-\pi}^{\pi}\frac{\mathrm{d}y}{2\pi}[\varphi]_{-l_x}^{l_x}, \tag{19}$$

The brackets in (18) and (19) denote the jump across the volume, $[f(x,y)]_{-l_x}^{l_x} = f(l_x,y) - f(-l_x,y)$. The first term on the right-hand side of (18) is the electromagnetic force acting in the y direction,

$$\begin{aligned}\frac{F_y}{\widehat{\beta}\rho_{\rm s}^2} &\equiv \frac{\widetilde{\psi}}{4\pi l_x}\int_{-l_x}^{l_x}\mathrm{d}x\int_{-\pi}^{\pi}\mathrm{d}y\, J\sin y,\\ &= \frac{\widetilde{\psi}}{4\pi C l_x}\int_{-l_x}^{l_x}\mathrm{d}x\int_{-\pi}^{\pi}\mathrm{d}y\,\nabla_\parallel(n-\varphi)\sin y.\end{aligned} \tag{20}$$

The last term in (18) represents the viscous force acting through the friction between the plasma and the wall.

An important consideration is the relationship between the phase velocity of the island in the frame where the plasma is at rest and the plasma flow velocity in the frame where the island is at rest. For $w \ll l_x$, the average velocity through the simulation domain $\bar{v}_y$ is approximately equal to the asymptotic velocity away from the island. Since the velocity of the plasma in the frame where the island is at rest is opposite to the velocity of the island in the frame where the plasma is at rest, it follows that the island velocity u satisfies $u \approx -\bar{v}_y$ (recall that with our normalization, the island velocity is equal to its frequency).

In steady state and for free propagation, the acceleration term $\mathrm{d}u/\mathrm{d}t$, the momentum source Γ_y and the electromagnetic force F_y must all vanish. It follows from (18) that the viscous force must also vanish in this case. The corresponding boundary condition is $v_y'(\pm l_x) = 0$. For numerical convenience, however, we use the alternative boundary condition $U(\pm l_x) = 0$ which is approximately equivalent to $v_y'(\pm l_x) = 0$ when $K \ll 1$. In order to satisfy the second condition, $F_y = 0$, we calculate the average flow velocity u such that this condition is satisfied by noting that at each time step, the new potential must be determined from the new vorticity by inverting $\nabla^2\varphi = U$. If φ_0 is the solution of $\nabla^2\varphi_0 = U$ such that $\varphi_0(\pm l_x) = 0$, the solution corresponding to average velocity $\bar{v}_y = -u$ is simply $\varphi = \varphi_0 - ux$. The value of u such that $F_y = 0$ is then simply

$$u = \frac{1}{2l_x\pi\widetilde{\psi}}\int_{-l_x}^{l_x}\mathrm{d}x\int_{-\pi}^{\pi}\mathrm{d}y\,\nabla_\parallel(\varphi_0 - n)\sin y. \tag{21}$$

This equation completes the specification of the boundary conditions for free propagation.

It is important to bear in mind that the condition $F_y = 0$ expresses only the lack of net external electromagnetic forcing. It does *not* signify equilibrium or local force balance. The numerical results described below clearly show that the island accelerates stochastically under the effect of turbulence even while $F_y = 0$ is satisfied.

System (14)–(15) is closely related to the Hasegawa–Wakatani model [15], from which it differs only by the presence of an island. Following Scott *et al* [16], we limit our simulations to two transverse dimensions. For a simple sheared slab the restriction to two dimensions has the result that the dynamics is characterized by a single resonant surface at $x = 0$, where $\nabla_\parallel = 0$. In the presence of an island, in contrast, the resonant surface is replaced by two neutral lines corresponding to the X-point and the O-point. The authors of [16] discuss extensively the role of the collisionality in a sheared field. They distinguish two regions. The first is a layer of width $\Lambda_\mathrm{d} = C^{1/2}$ around the resonant surface. They call this layer the hydrodynamic region. In the hydrodynamic region $k_\parallel$ is small so that the turbulence is unaffected by the magnetic field and the vorticity is governed by Euler's equation. The second region consists of the exterior of the layer where $k_\parallel$ is large so that the density obeys Boltzmann's law, $\widetilde{n} \cong \widetilde{\varphi}$. In the exterior region the vorticity is governed by the Hasegawa–Mima equations [17]. Similar regions also appear in our system where, because of the island, the parallel wave number is a function of both the radial and transverse coordinate, $k_\parallel = k_\parallel(x, y)$.

An important property of system (14)–(15) is the existence of an exact stationary solution for $\varphi = n = -x$ (corresponding to an island rotating at the electron diamagnetic frequency, $u = 1$). This equilibrium has the remarkable property of existing for an arbitrary choice of all the parameters including w. We will thus refer to it as the universal root. Numerical and analytical investigations show that the equilibrium problem can also present other roots [18–21].

3. Linear stability

We begin the study of the system by analyzing its linear stability with respect to the drift-wave perturbations. It is well known that in order to have self-sustained turbulence and mode coupling, a sufficiently large number of linearly unstable modes is required. The presence of a radial density gradient can destabilize resistive drift waves and therefore provide a drive for the electrostatic turbulence. These instabilities can be damped by a sufficiently large dissipation, represented in our model by the ion viscosity and the particle diffusion.

It is important to note that we will encounter three different types of instabilities in this paper. Besides the drift and interchange modes (micro-instabilities) examined in this section we will also consider the stability of the tearing mode (macro-stability, i.e. the growth or healing of the island) and, in the case of free islands, the stability of the roots for the propagation frequency (as an example of a familiar propagation instability we cite mode locking, although we will not consider that particular instability here). In order to distinguish between the three types of instability, we will reserve the word '*stability*' (without adjectives) to describe stability with respect to drift-wave perturbations. Therefore, with this convention a stable system is quiescent, while an unstable one is turbulent. We will refer to the stability of the tearing mode as '*magnetic stability*' or equivalently '*tearing stability*'. Lastly, we will describe the stability of the propagation roots by the term '*rotational stability*'.

The linearized version of equations (14)–(15) is solved with a finite-difference numerical code (benchmarked with analytical solutions [22, 23]). The generic perturbation $\widetilde{f}$ is assumed to have the form: $\widetilde{f}(x, y, t) = \widetilde{f}(x) \sum_m \exp[\mathrm{i}(my - \omega t)]$. The real part of ω gives the rotation

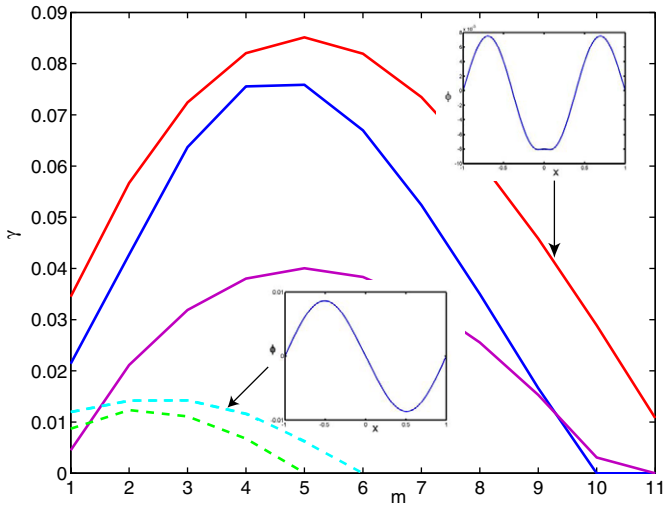

Figure 1. Dispersion relation of the resistive drift waves for $D = \mu = 0.022$. The solid and dashed lines are related to even and odd eigenfunctions, respectively. The insets show the wavefunctions for the indicated branches.

frequency of the mode, while $\gamma = \Im(\omega) > 0$ corresponds to a growing perturbation. For $w = 0$, i.e. for a sheared magnetic field without island, the linearization of equations (14)–(15) yields

$$\mathrm{i}\omega\left(\frac{\partial^2\widetilde{\varphi}}{\partial x^2} + m^2K^2\widetilde{\varphi}\right) = -\frac{m^2x^2}{C}(\widetilde{n} - \widetilde{\varphi}) - D\left(\frac{\partial^2\widetilde{n}}{\partial x^2} - m^2K^2\widetilde{n}\right), \tag{22}$$

$$\mathrm{i}\omega\widetilde{n} + \mathrm{i}\omega_*\widetilde{\varphi} = \frac{m^2x^2}{C}(\widetilde{n} - \widetilde{\varphi}) - \mu\left(\frac{\partial^4\widetilde{\varphi}}{\partial x^4} - \mathrm{i}m^2K^2\frac{\partial^2\widetilde{\varphi}}{\partial x^2} + m^4K^4\widetilde{\varphi}\right), \tag{23}$$

where the generic equilibria n_{eq} and φ_{eq} are a function of the radial coordinate only and the prime represents differentiation with respect to x.

For the sake of simplicity, we take the Schmidt number $\mu/D = 1$ throughout this paper. We further restrict attention to the case $C = 1$, which is a representative value for the edge of fusion experiments, and fix $K^2 = 0.0225$. It follows that when $w = 0$, only two parameters regulate the stability properties of the plasma: the normalized dissipation ($D = \mu$) and the azimuthal wave number of the drift-wave perturbation, m.

We define the *reference equilibrium* as the state corresponding to the universal root, $\varphi_{\mathrm{eq}} = n_{\mathrm{eq}} = -x$, for a sheared magnetic field with no island. Note that the linear stability is independent of the background poloidal velocity. That is, a constant value of φ'_{eq} corresponds to a constant Doppler shift in the rotation frequency and does not affect the growth rate of the mode.

In order to establish the properties of the turbulence as a function of our chosen parameters we solve numerically the eigenvalue problem defined by equations (22)–(23) for different values of $D = \mu$ and examine the features of the unstable modes. Figure 1 shows the dispersion relation, i.e. it shows the graphs of the growth rates as a function of the azimuthal wavenumber m for the five different radial eigenmodes that have positive growth rates at $D = \mu = 0.022$. These eigenmodes differ from each other by their spatial structures, two of which are shown in the insets. The even (interchange parity) and odd (tearing parity) modes have qualitatively different dispersion relations (that is, different graphs of γ versus m). The unstable band for

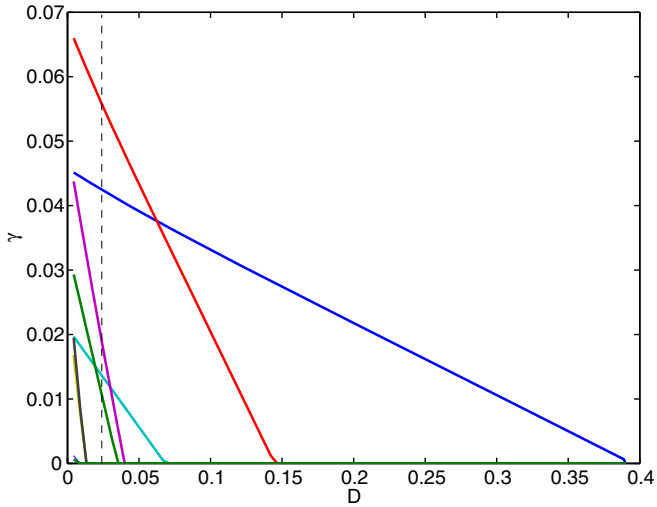

Figure 2. Growth rates of the $m = 2$ unstable resistive drift waves as a function of $D = \mu$, showing the stabilizing effect of dissipation. The dashed line shows the value of $D = \mu$ used in figure 1.

even modes extends to much higher azimuthal wavenumbers m, and their growth rate peaks at higher m than the odd modes. The growth rate of the most unstable even modes is greater than that of the odd modes at all m, and their peak growth rate exceeds that of the odd modes by almost an order of magnitude.

We next consider the effect of the dissipation described by $D = \mu$. We find that dissipation has a stabilizing effect on both even and odd modes, as might have been expected. As D rises, odd modes are the first to be stabilized (figure 2). We denote the threshold for stabilization of the odd modes by $D = D_{\text{odd}}$. A second threshold $D = D_{\text{evn}} > D_{\text{odd}}$ denotes the value of dissipation above which all even modes are stable. In the region $D_{\text{odd}} < D < D_{\text{evn}}$ only even (interchange-parity) modes are unstable. Since the parity of the background ($m = 0$) fields is odd, it is possible to suppress the turbulence in the region $D_{\text{odd}} < D < D_{\text{evn}}$ by numerically enforcing odd parity. This is a very important property as it provides a means of comparing turbulent and quiescent states with identical values of *all* the parameters. Other means of quelling the turbulence, such as increasing D, have effects on the background equilibrium that are difficult to distinguish from the effects of the turbulence.

A key question is how the presence of an island modifies the linear stability properties of drift waves described above. A well-known effect of magnetic islands is the tendency for the profiles of density and pressure to flatten inside the separatrix [19, 26, 27]. Since the radial gradient of the background density is the source of free energy for the drift-wave instability, one expects the local flattening caused by the presence of an island to have a stabilizing effect on the turbulence. In order to quantify the consequences of this stabilizing effect without carrying out a 2D stability analysis, we have investigated equilibria with a 1D radial density profile, $n_{\text{eq}}(x)$, that is partially flattened in a region of width w around the neutral line. We have used the model family of profiles

$$n_{\text{eq}}(x) = -x + (1 - \omega_{*0})x\mathrm{e}^{-2(x/w)^2}, \tag{24}$$

where ω_{*0} represents the local diamagnetic frequency at the O-point. This family of profiles, shown in figure 4 can be thought as an average over y of the actual 2D flattened profile. In self-consistent nonlinear simulations, we expect that the degree of density flattening ω_{*0} will

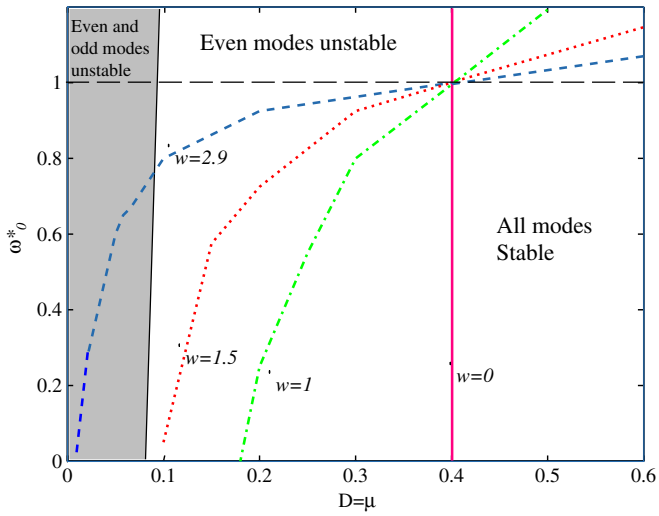

Figure 3. Stability thresholds for the even and odd modes. The shaded region represents the domain of instability of the odd modes and the thin, nearly vertical line bordering this shaded region represents $D_{\rm odd}(\omega_{*0}, w)$, which depends very weakly on w as well as ω_{*0}. The remaining lines represent $D_{\rm evn}(\omega_{*0}, w)$ for $w = 0$ (vertical solid line), $w = 1$ (dashed–dotted line), $w = 1.5$ (dotted line) and $w = 2.9$ (dashed line). The dashed horizontal line shows the unperturbed background electron diamagnetic frequency.

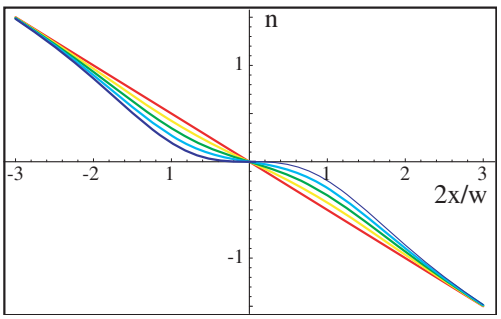

Figure 4. Density profiles corresponding to the model described by equation (24). The five curves correspond to local diamagnetic frequencies ω_{*0} ranging from 0 (fully flattened) to 1 (unperturbed profile), and the radial variable is normalized to the half-width of the island.

depend on the island width as well as the other parameters. Since this dependence is unknown *a priori*, however, we will treat ω_{*0} as an independent parameter in this section.

Figure 3 shows the dependence on D, for selected values of w, of the critical inner density gradients $\omega_{*0}^{\rm odd}$ and $\omega_{*0}^{\rm evn}$ for marginal stability against odd and even modes. This figure shows that the stabilization threshold for the even modes, $\omega_{*0}^{\rm evn}(D; w)$, depends sensitively on the dissipation D, the sensitivity becoming greater as the island width increases. The stabilization threshold for the odd modes, $\omega_{*0}^{\rm odd}(D; w)$, is even more sensitive to D. In fact, the stability boundary for the odd modes is best characterized in terms of the critical diffusion $D_{\rm odd}$, which is almost independent of ω_{*0} because these unstable modes and the flattened component of the equilibrium field share the same parity.

In summary, we have performed a complete scan in w, ω_{*0} and $D = \mu$ in order to determine the stability of the system. We find that for $w \neq 0$ the stability of the drift waves is determined

by the island width w (the width of the flattened region) and the locally reduced diamagnetic drift frequency ω_{*0} (measuring the amount of density flattening) in addition to the parameters that we considered earlier in the $w = 0$ case (the wave number m of the perturbation and the dissipation $D = \mu$).

4. Nonlinear results

In this section we describe the results obtained in the nonlinear regime, where mode coupling produces turbulent cascades and other transfers of energy and enstrophy between the modes [8, 16]. We examine, in particular, the effect of the turbulence on the magnetic island. This effect is mediated by the polarization currents.

Our study uses an initial-value, finite-difference code [20, 24] to solve numerically system (14)–(15) (completed by the boundary condition $u = \text{const}$ or $F_y = 0$). The code uses a fully implicit multi-grid algorithm (4th order in space and 2nd order in time) constructed using Portable Extendible Toolkit for Scientific Computation (PETSc). The size of the numerical box is $[-l_x : l_x, -\pi : \pi]$ with $l_x = 6.7$ and the grid resolution is 100×112 points.

In the nonlinear phase, the response of the plasma to the presence of an island includes a combination of ion polarization currents and currents associated with external electromagnetic forces (when such forces are present). The currents can be laminar or turbulent, depending on the parameters. When the system evolves from a quiescent to a turbulent state, however (as a result of a decrease in the dissipation, for example), the large-scale, slowly evolving plasma response coexists with, and is partly driven by, the turbulent fluctuations. Since our main concern is to describe how the turbulence interacts with the magnetic island, we need to separate the effect of the laminar component of the flows from that of the turbulent fluctuations. In order to do that we begin by examining, for different island widths and rotation frequencies, the reference states obtained by suppressing the turbulence.

4.1. Reference states

The reference states are quiescent, fully relaxed ($\partial/\partial t = 0$) solutions that result from enforcing odd parity of the fields ϕ and n for values of the parameters D, w and u such that the odd eigenmodes are stable (see section 3). In the following we describe the properties of these reference states:

In figure 5 we plot the azimuthal force $F_y/(\widehat{\beta}\rho_s^2)$ and tearing stability parameter $\Delta_{\text{pol}}\rho_s/\widehat{\beta}$ as a function of the imposed average azimuthal frequency u for $w = 2.9$ and several values of the dissipation $D = \mu$. Recall that the roots of $F_y = 0$, given by the intersections of the force curve with the abscissa, represent freely propagating islands. We see that as the dissipation decreases, the number of free-propagation roots increases. For $D = 0.6$ (uppermost curve) the only root is the universal solution $u = 1$, corresponding to the solution $\varphi = n = -x$. Between $D = 0.6$ and $D = 0.4$, however, a tangent bifurcation takes place leading to the emergence of an additional pair of roots with velocities below the drift frequency at $u \simeq 0.75$ and $u \simeq 0.85$. Between $D = 0.2$ and $D = 0.1$ a second tangent bifurcation leads to the emergence of yet another pair of roots at still lower propagation frequency. The lowermost curve corresponding to $D = 0.1$ thus exhibits no less than five free-propagation roots. The *rotational* stability of the multiple roots can be determined by evaluating the derivative of the force with respect to the frequency, with $\mathrm{d}F_y/\mathrm{d}u < 0$ and $\mathrm{d}F_y/\mathrm{d}u > 0$ indicating that the root is, respectively, *rotationally* stable and unstable with respect to small perturbations of u.

The bottom graph in figure 5 shows the island (macroscopic) stability parameter Δ_{pol}, as a function of the azimuthal frequency. We see that for the larger values of the dissipation, the

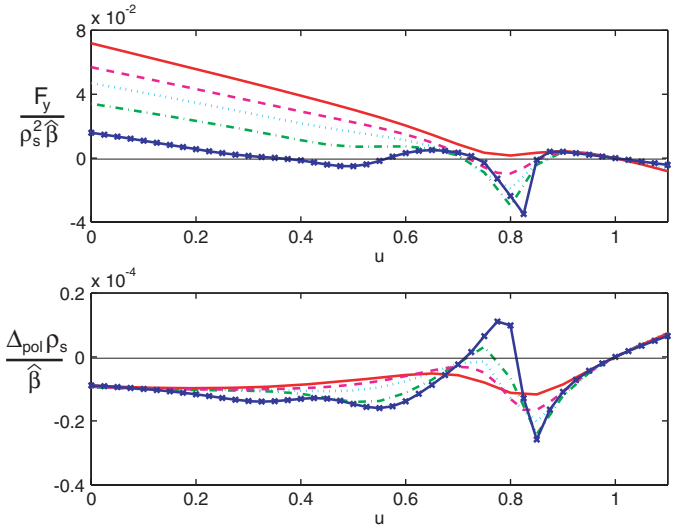

Figure 5. Effect of the dissipation on the reference states with $C = 1$ and $w = 2.9$. The curves represents different values of $D = \mu$: 0.1 solid with crosses, 0.2 dash–dot, 0.3 dots, 0.4 dash, 0.6 solid.

polarization current is stabilizing ($\Delta_{\rm pol} < 0$) whenever the island propagates more slowly than the electron diamagnetic frequency, in agreement with previous investigations [20, 25]. For very small dissipation, $D < 0.2$, a window in propagation frequency appears (approximately in the range $0.7 \lesssim u \lesssim 0.8$) where the polarization drift is destabilizing. This is consistent with the results of simulations using a kinetic model for the ions (corresponding to $D = \mu = 0$) that show the existence of magnetically unstable bands for $u < 1$ [12]. We note that the free-propagation roots lie at the periphery of the magnetically unstable band, so that the drive for the tearing mode is weak. Nevertheless, the occurrence of magnetic destabilization raises the question of the effect of the island width on propagation frequency and magnetic stability. We next address this question.

Figure 6 shows the dependence of the free-propagation frequency u on the width of the island for $D = \mu = 0.1$ and $C = 1$. The thick solid and dashed lines represent *rotationally* stable and unstable islands respectively. The shaded areas correspond to the regions where $\Delta_{\rm pol}$ is positive and consequently the polarization currents flowing in the system induce a *magnetic* destabilization of the island. Figure 6 thus constitutes a diagram summarizing the rotational as well as the magnetic stability of the island. This diagram makes it possible to predict the evolution of the island parameters w and u given a set of initial conditions.

The structure of the stability diagram reveals the possibility of slow oscillations between bistable states. To see this, consider the evolution of an island for $\Delta' = 0$. Figure 6 shows that an island initialized with a small amplitude $w \simeq 0.5$ in the tearing-unstable region corresponding to $u \simeq 0.75$ will initially grow and slow down slightly, until it reaches the tangent bifurcation for $w \cong 3.25$. At this critical point, a further increase in the island width results in a transition to a new root with slower rotation. For the new root the polarization current is *magnetically stabilizing*, so that the island heals. When the w reaches the second tangent bifurcation at $w \cong 2.6$, however, the system makes a reverse transition to the original branch, closing the hysteretic cycle. We have thus shown that the island width and rotation frequency will oscillate when Δ' is smaller than the absolute value of $\Delta_{\rm pol}$ calculated at the second bifurcation point.

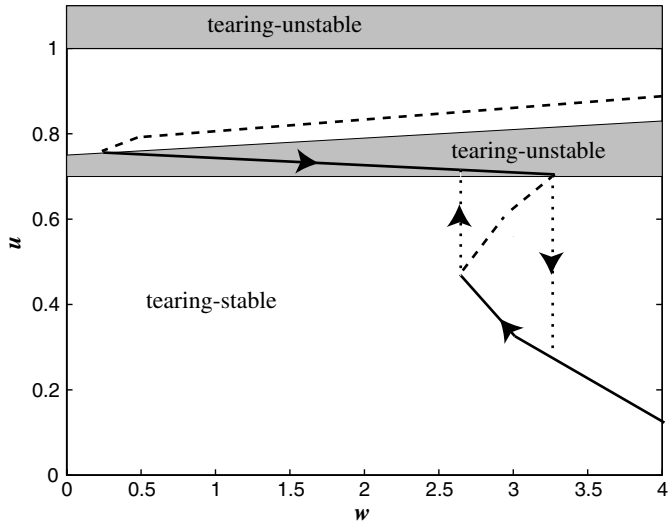

Figure 6. Relation between the unforced ($F_y = 0$) quiescent island width, w, and rotation frequency, u, for reference states with $D = \mu = 0.1$ and $C = 1$. The solid and dashed lines represents *rotationally* stable and unstable roots, respectively, while the shaded areas are associated with a positive (*magnetically* destabilizing) $\Delta_{\rm pol}$.

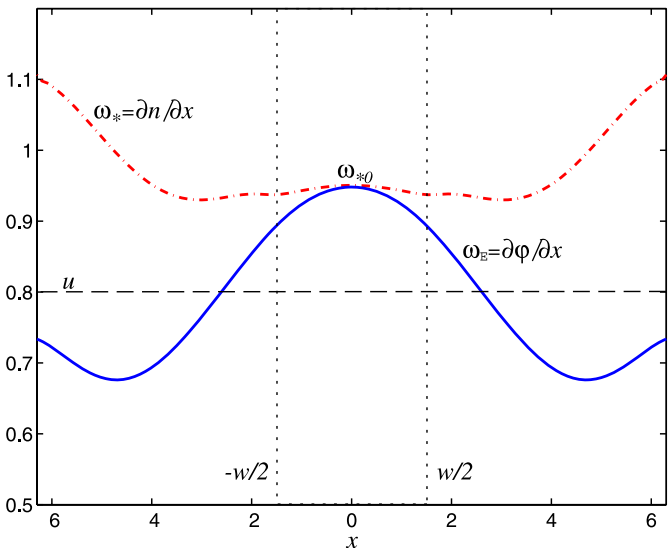

Figure 7. Profiles of the electric drift frequency and the diamagnetic drift frequency for $C = 1$ and $w = 2.9$. The dashed line represents the value of the average flow imposed through the boundary condition.

In the opposite limit, when Δ' exceeds this value, the island will reach a stationary saturation on the third root branch. Of course, the above picture depends on the dissipation D and μ. As the dissipation increases the cycle gets smaller and eventually disappears.

An important property of magnetic islands is the relationship between the flattening of the density inside the island and the rotation frequency of the island. Figure 7 shows the profile

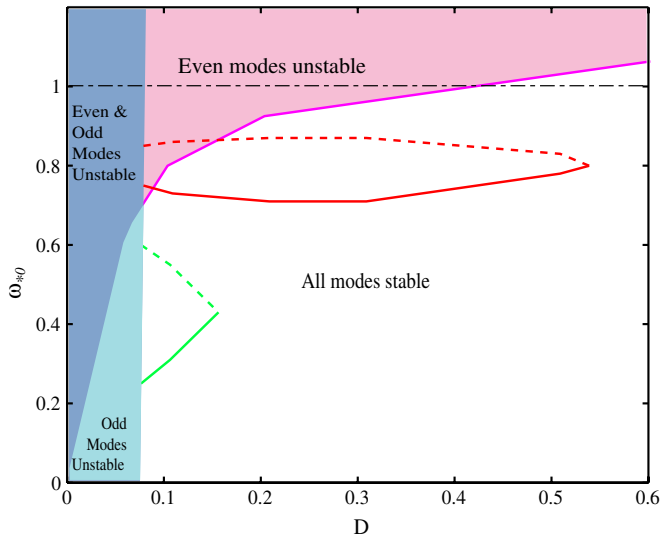

Figure 8. Regions of stability of the even and odd drift waves as a function of D and ω_{*0} for $w = 2.9$. On the same plot we use the approximate relation $u = \omega_{*0}$ to represent the roots of $F_y = 0$ as a function of ω_{*0} and $D = \mu$ for reference states. Rotationally stable (unstable) unforced solutions are represented with solid (dashed) lines.

of the electric drift frequency $\partial\varphi/\partial x$ and of the diamagnetic frequency $\partial n/\partial x$ across the O-point of a reference-state island as well as the imposed average rotation frequency (dashed horizontal line). The figure shows that in the center of the island the electric drift approximately compensates the diamagnetic drift, so that the electrons are at rest in a frame moving with the island. This is a manifestation of the frozen-in property preventing the electrons from crossing flux surfaces and, in particular, the separatrix. The applicability of the frozen-in property may seem surprising given the use of $C = 1$ in our simulations. Inspection of Ohm's law, however, shows that it is the product CJ that must be small,

$$\nabla_\parallel (n - \varphi) = CJ \ll 1,$$

so that the electrons are frozen-in whenever $J \ll 1$, a condition that is satisfied *for the long wavelength components* in all our simulations since $J \sim \Delta' W \ll 1$.

Consistent with the frozen-in property, all the states with $u < 1$ show a partial density flattening in the island region. The flattening becomes more pronounced for slower and wider islands. We note that the fields associated with the solutions such that $u < 1$ are delocalized. That is, the island excites propagating drift waves [28]. The radial wavevector for these waves is $k_x(x) = \sqrt{1 - \omega_*(x)/u}$. They are most strongly excited when $k_x w \sim 1$. Note, however, that the density flattening inhibits wave excitation and propagation by enforcing $u \simeq \omega_*(0)$.

We may use the frozen-in property, $u \simeq \omega_*(0)$, to draw the locus of unforced ($F_y = 0$) solutions of the quiescent nonlinear simulations in the linear stability diagram of figure 3. The result is shown in figure 8 for $w = 2.9$. The solid and the dashed lines in this diagram represent the frequency of the roots of $F_y = 0$ in figure 5 corresponding, respectively, to *rotationally* stable and unstable propagation for the case with enforced parity. These lines lie mostly in the regime where resistive drift waves are stable, reflecting the stabilizing effect of density flattening. The two higher-frequency roots, however, cross the stability limit for even modes at $D \approx 0.16$ and $D = 0.09$. We thus expect turbulence to develop in these states when both parities are allowed to evolve. We examine the effects of turbulence next.

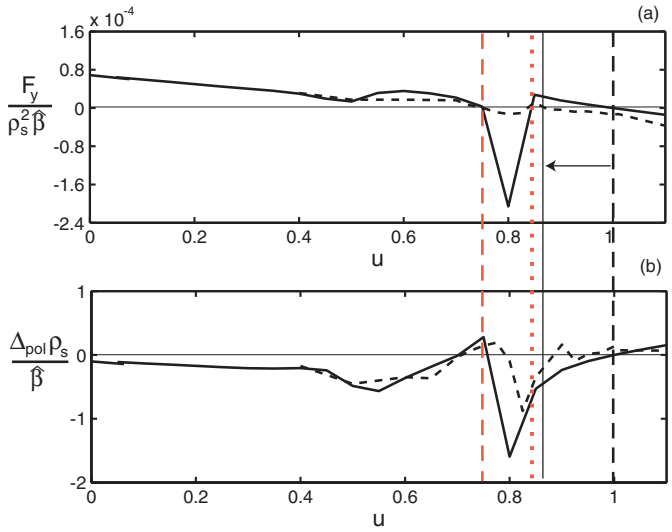

Figure 9. (*a*) Perpendicular force $F_y/(\widehat{\beta}\rho_s^2)$ acting on the island and (b) *magnetic* stability parameter $\Delta_{\rm pol}\rho_s/\widehat{\beta}$ versus imposed frequency u for $w = 0.5$. The solid lines represent quiescent states (parity enforced numerically) and the dashed lines are the time-averaged values in the turbulent states. The vertical dashed (dotted) lines indicate rotationally stable (unstable) unforced states for the quiescent island, and the thin vertical solid line represents the position of the displaced 'universal' root in a turbulent island.

4.2. Turbulent regimes with forced rotation

We now turn to the discussion of the results obtained in the turbulent regime that develops when the parity enforcing constraint is released. In order to excite all the degrees of freedom of the system and to reduce the computational time necessary to reach saturation, the nonlinear code is initialized with adiabatic turbulence, with amplitude spectrum $|n_k| \propto k^2/(1+k^4)$ and random phase. The seed turbulence is localized in the central region of the numerical box by using a spatial Gaussian envelope with amplitudes in the linear regime.

In order to gain some understanding of the problem, we first investigate the response of the system for an imposed average flow $u =$ constant. Figures 9–12 show two quantities as a function of u: the normalized polarization drive $\Delta_{\rm pol}\rho_s/\widehat{\beta}$ and the external forcing, $F_y/(\widehat{\beta}\rho_s^2)$. The solid lines show these two quantities for quiescent states, and the dashed lines show the *time average* of the same two quantities for turbulent states. The four figures correspond to different values of the island width, namely $w = 0.5$, 1.5, 2.9 and 4.1. For all these figures, $D = \mu = 0.1$ and $C = 1$.

We see that the dashed (turbulent) and solid (quiescent) lines overlap when the island is rotating sufficiently slowly, in agreement with the fact that the turbulence can develop only if $\omega_{*0} > \omega_{*0}^{\rm evn}$ (as described in section 3). When the two curves separate, their difference corresponds to the net effect of the turbulence *at fixed frequency*.

The tearing stability curves in figures 9(*b*), 10(*b*), 11(*b*) and 12(*b*) show that over most of the range of parameters resulting in turbulence, the turbulent states have somewhat higher $\Delta_{\rm pol}$ than the states with laminar flow. This leads to the conclusion that *at fixed frequency* the effect of turbulence is to drive island growth. This conclusion may be significant in the context of the efforts to mitigate edge localized modes by creating a stochastic region at the edge with resonant magnetic perturbations. Turbulent amplification of the perturbations, if confirmed with more detailed models of the turbulence, would facilitate island overlap.

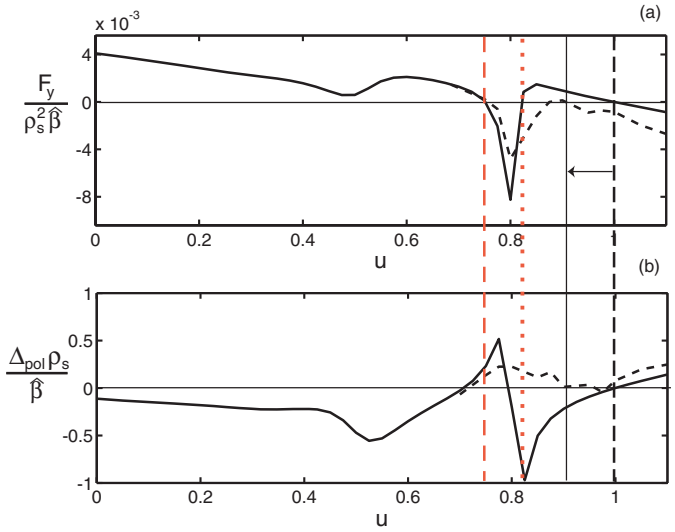

Figure 10. Same as figure 9 but for $w = 1.5$.

An exception to the destabilizing influence of turbulence at fixed frequency occurs near the resonances of the quiescent $\Delta_{\rm pol}$ (e.g. the sharp peak in $\Delta_{\rm pol}$ at $u \approx 0.75$ in figure 10(b)). We see that the turbulence has a smoothing effect on these resonances that can be stabilizing for nearby values of u. The resonances are associated with the matching of the radial wavelength of the drift waves with the width of the island, corresponding to $k_x w \simeq 1$. This allows for the formation of a standing drift wave near the island [12]. The diffusive effect of the turbulence on the resonances may thus represent a form of resonance broadening.

The preceding discussion addressed the case of externally driven islands, where the propagation velocity is fixed. In the case of free propagation, in contrast, it is necessary to account for the effect of the turbulence on the island's propagation frequency. Indeed, inspection of the force curve shows that turbulence changes the roots of $F_y(u, w) = 0$ qualitatively. The vertical dashed and dotted lines in figures 9(a), 10(a), 11(a) and 12(a) indicate the velocities corresponding to free rotation in the *reference* state. The free rotation solutions in the turbulent states are dramatically different. The universal root, in particular, shifts from its value of $u = 1$ in quiescent plasma to a much smaller value near $u \simeq 0.85$. The precise new value of the root depends on the parameters, so that it clearly can no longer be called 'universal.' Furthermore, it survives only as a very weak root in the sense that it is very close to the next, rotationally unstable root. In other words, it is nearly a double root. Figures 11(a) and 12(a) shows that between $w = 2.9$ and $w = 4.1$ the two nearby roots merge and disappear altogether. The effects of turbulence on the universal root are unsurprising when one considers that this solution root is also lost in models that retain the effects of sound waves [20, 29]. We note that another interesting feature of the force curves for the reference states (solid lines) is the merger and disappearance of the second and third (from the left) roots for free propagation as the island width grows from $w = 2.9$ to $w = 4.1$ in figures 11(a) and 12(a). This merger corresponds to the bifurcation point at $w = 3.25$ and $u = 0.75$ in figure 6.

A simple model for the effect of noise on the electromagnetic force curve sheds some light on the effect of the mechanism whereby turbulence modifies the free-propagation roots. Consider a stochastic perturbation of the frequency, $\widetilde{u}(t)$. If u_0 is the natural velocity in the quiescent state, $F_y(u_0) = 0$, the averaged value of the transverse force in the presence of the

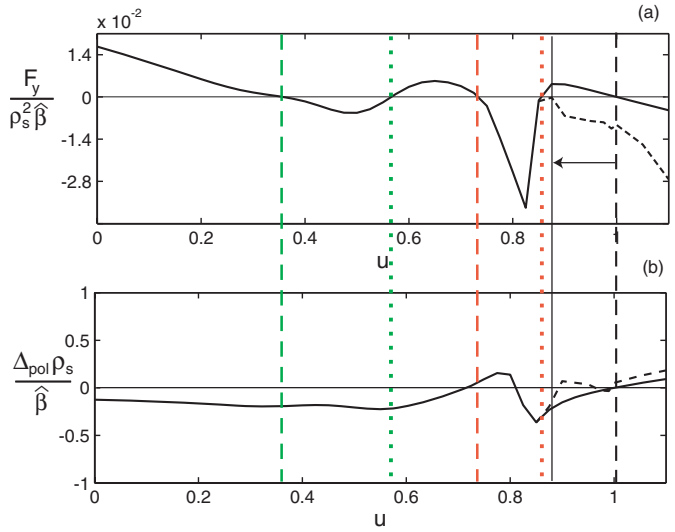

Figure 11. Same as figure 9 but for $w = 2.9$.

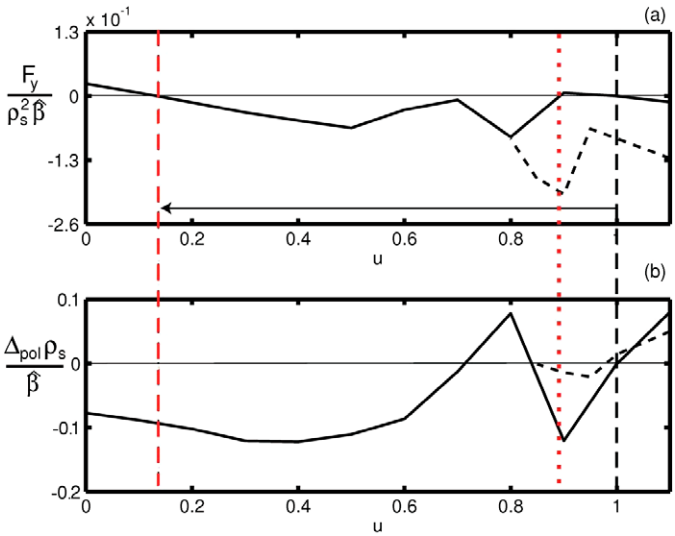

Figure 12. Same as figure 9 but for $w = 4.1$.

stochastic perturbation is

$$\overline{F_y(u_0 + \widetilde{u}(t))} = F_y''(u_0)\overline{\widetilde{u}(t)^2} + O(\overline{\widetilde{u}^4}). \tag{25}$$

We see that the noise exerts a drag-force on the island if $F_y''(u_0) < 0$. The interested reader will find a more sophisticated analysis of the effects of fluctuations on island growth in the paper by Itoh *et al* [10].

In summary, we see that the most salient effect of turbulence is to cause transitions by modifying the unforced states available to the island. As a result, turbulence can change qualitatively the effective $\Delta_{\rm pol}$ experienced by an island even when it has only a modest effect

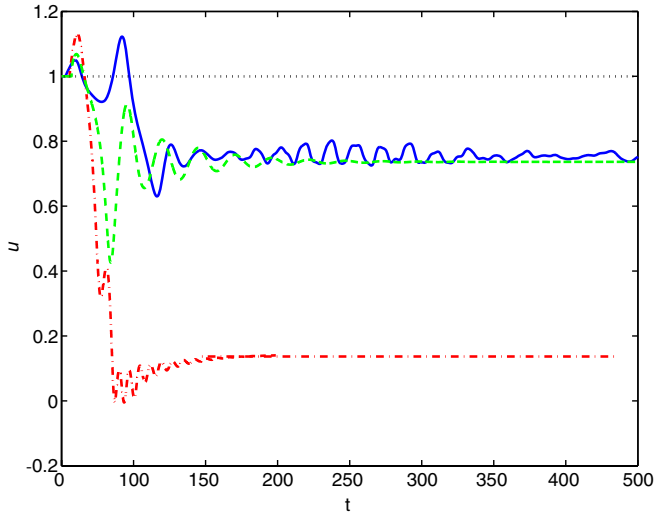

Figure 13. Time evolution of the frequency for $w = 0.5$ (solid line), $w = 2.9$ (dashed line), and $w = 4.1$ (dashed–dotted line).

on $\Delta_{\rm pol}$ at fixed frequency. In particular, for $w = 0.54$ and $w = 2.9$, the shift of the 'universal' root from $u = 1$ to $u \simeq 0.85$ has a *stabilizing* effect on the island since $\Delta_{\rm pol} < 0$ for the modified root. For $w = 4.1$, the annihilation of the remnant of the universal root leads the frequency to drop to $u \simeq 0.15$ where $\Delta_{\rm pol}\rho_{\rm s}/\hat{\beta} \simeq -0.1$ is stabilizing.

We will see in the following section that the simulations with free rotation are qualitatively consistent with the picture drawn from the analysis of the fixed rotation case. They provide useful information, however, on the dynamical behavior of the island rotation.

4.3. Turbulent regimes with free rotation

In order to investigate the transitions in the rotation frequency of the tearing mode, we have adjusted the boundary condition on φ every time step in such a way that throughout the evolution $F_y = 0$. Figure 13 shows the evolution of the rotation frequency for islands initialized with $u = 1$. With enforced parity the rotation frequency remains fixed at $u = 1$ (dotted line). When we allow the turbulent fluctuations to develop, in contrast, the island slows down abruptly. For $w = 0.5$ (solid line), the frequency settles in a turbulent steady state around the root at $u \approx 0.75$, overshooting the displaced 'universal' root at $u \approx 0.85$. Figure 9(*b*) shows that $\Delta_{\rm pol}\rho_{\rm s}/\widehat{\beta} > 0$ for that root so that the transition increases the drive for the nonlinear tearing mode. For $w = 2.9$ (dashed line), the final rotation frequency is similar to that for $w = 0.5$ but the density flattening now extends over the entire hydrodynamic region ($w > C^{1/2} = 1$) with the result that the resistive drift waves are stable and the final state is quiescent. Figure 11(*b*) shows that $\Delta_{\rm pol}\rho_{\rm s}/\widehat{\beta} \approx 0$ for the final state, so that the transition has a negligible effect on the drive. Lastly, for $w = 4.1$ (dashed–dotted line) the intermediate unforced roots have disappeared through merging and the island slows to the smallest root at $u \approx 0.15$. In this state the polarization current is *magnetically stabilizing* and the plasma is quiescent.

5. Interchange instability

In this section we investigate how the presence of an unfavorable curvature can affect the interaction between the turbulence and the magnetic island. The extended version of our

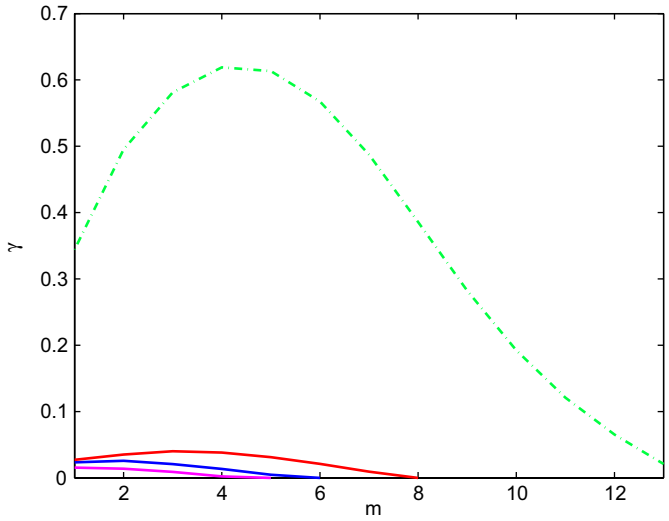

Figure 14. Dispersion relation of the resistive drift waves (solid lines) and interchange instability (dash–dot line) for $D = \mu = 0.022$, $C = 1$ and $G = 0.45$.

theoretical model equations (14)–(15) now reads

$$\frac{\partial U}{\partial t} + \boldsymbol{v} \cdot \nabla U = \frac{1}{C}\nabla_{\parallel}^2(n - \varphi) + G\partial_y n + \mu\nabla^2 U, \tag{26}$$

$$\frac{\partial n}{\partial t} + \boldsymbol{v} \cdot \nabla n = \frac{1}{C}\nabla_{\parallel}^2(n - \varphi) + G\partial_y(n - \varphi) + D\nabla^2 n, \tag{27}$$

where the new terms are proportional to $G = 2q\rho_s\sqrt{\beta}/\omega_* = 2qL_n/L_s$ (q is the safety factor).

In the system thus modified, interchange modes can become unstable and therefore provide a new drive for the turbulence. The numerical analysis of the linear version of equations (26)–(27) shows that the interchange modes are unstable when $0 \lesssim G \lesssim 1$ and their average growth rate reaches a maximum for $G \cong 0.45$ (for a theoretical treatment see also [23]). Moreover, as shown in figure 14 for $D = \mu = 0.022$, $w = 0$ and $C = 1$, the curvature terms also affect the drift-wave dispersion relation, reducing their growth rate. Note that the eigenfunctions of φ and n associated with the interchange mode are even with respect to x and therefore, also in this case, the instability can be eliminated by enforcing parity.

Figure 15 shows the reference states for different values of G. Note that the universal root is a rotationally stable quiescent equilibrium also for system (26)–(27). Increasing G, the unforced delocalized root disappears while the rotation frequency associated with the unforced localized solution becomes smaller. At the same time, $\Delta_{\rm pol}\rho_s/\widehat{\beta}$ becomes positive for small u, resulting in an island growth for the $F_y = 0$ solution.

In figure 16 we show the effect of the turbulence generated by the interchange instabilities on a magnetic island of width $w = 1.5$ for $G = 0.45$ and the other physical parameters as in figure 15. Remarkably, the stronger G-mode drive is never completely quenched by the flattening of the island and therefore the turbulence survives also when the island rotates very slowly. As a comparison, for the case $G = 0$ and the same island width, the drift-wave turbulent fluctuations were completely suppressed for $u \lesssim 0.7$. It is interesting to note that the rotation frequency of the slow solution ($u \simeq 0.1$) is not significantly affected by the electrostatic fluctuations. At the same time, the value of $\Delta_{\rm p}\rho_s/\widetilde{\beta}$ is reduced by almost 50%, thus implying that the turbulence has a *magnetic* stabilizing effect.

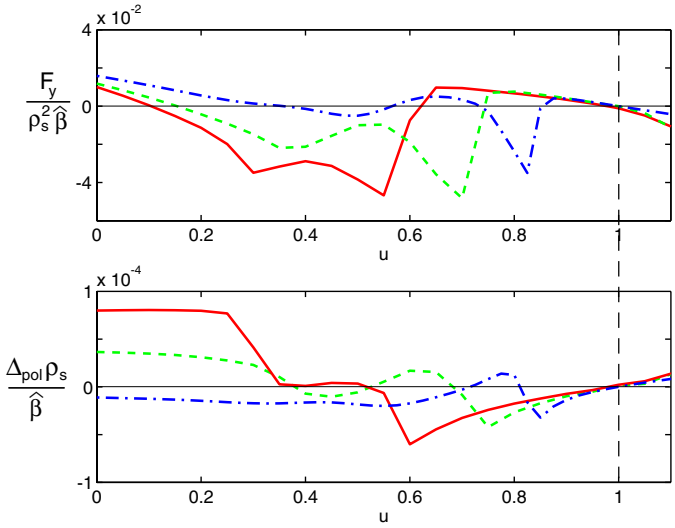

Figure 15. Effect of the curvature on the reference states with $D = \mu = 0.1$, $C = 1$ and $w = 2.9$. The curves represent different values of G: 0 (dash–dot), 0.225 (dash), 0.45 solid.

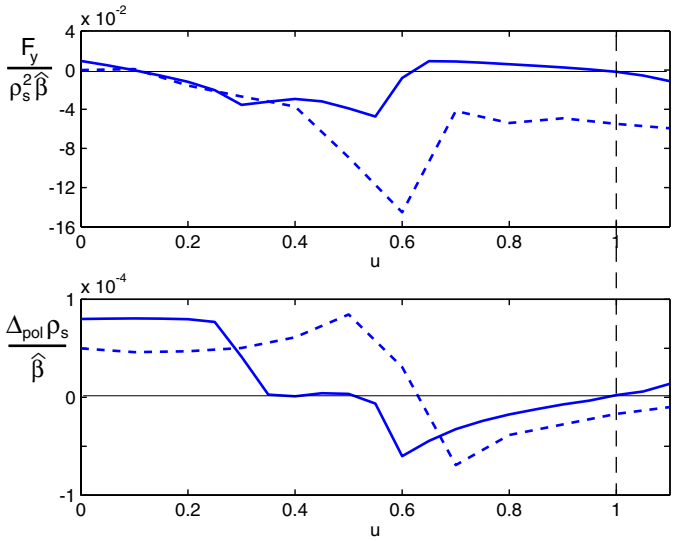

Figure 16. Perpendicular force $F_y/(\widehat{\beta}\rho_s^2)$ acting on the island and *magnetic* stability parameter $\Delta_{\rm pol}\rho_s/\widehat{\beta}$ versus imposed frequency u for $w = 2.9$, $C = 1$, $G = 0.45$ and $D = \mu = 0.1$. The solid lines represent quiescent states (parity enforced numerically) and the dashed lines are the time-averaged values in the turbulent states.

6. Summary and conclusions

In low-β plasmas magnetic islands coexist and interact with mostly electrostatic plasma turbulence. The model presented in this paper describes the interaction between electrostatic fluctuations and magnetic perturbations that can be represented with the constant-$\widetilde{\psi}$ approximation ($\widehat{\beta} \ll 1$). The magnetic island is assumed to evolve more slowly than the

surrounding turbulence, thus allowing for an electrostatic treatment of the long wavelength as well as the short wavelength modes.

In a simple model without magnetic islands, the transition of the background fields from a completely quiescent to a turbulent state is regulated only by the competition between the dissipation present in the system, such as the particle diffusion or the ion viscosity, and the free-energy source given by the density gradient. The picture is more complex when the system includes a magnetic island, which can yield significant modifications of the spatial structure of the density profile. In particular, the topology of the reconnected magnetic field can induce a reduction of the instability drive through the flattening of the density inside the separatrix.

As a guide in understanding the nonlinear simulations, we have carried out a systematic numerical investigation of the linear behavior of the drift-wave instabilities in the presence of a magnetic island. We find that the flattening of the density profile associated with slowly rotating, large islands is effective in quenching the drift-wave modes with even parity with respect to the radial coordinate. Furthermore, for different island amplitudes, we identify a region in the $D - \omega_0$ space where only even modes are excited. We use this to compare turbulent simulations to quiescent runs obtained with the same parameters by eliminating the turbulence through parity enforcement.

We find that the drift-wave turbulence affects the magnetic island dynamics through the polarization current. The polarization current in the presence of turbulence differs from that in quiescent simulations in several respects. In particular, the turbulence generates zonal flows [30, 31] that affect the torque balance (through their effect on momentum transport) and therefore contribute in the definition of the rotation frequency of the magnetic perturbation. The parameters $\Delta_{\rm pol}\rho_{\rm s}/\widehat{\beta}$ and $F_y/(\widehat{\beta}\rho_{\rm s}^2)$ quantify the effect of the turbulence on the island. These parameters specify the values of the external drive Δ' for the tearing mode and the momentum source Γ_y required to sustain the island at the imposed width, w, and rotation frequency, u.

For a fixed w, the multiplicity of the roots associated with unforced islands increases by reducing the value of the dissipation, passing from a single trivial quiescent solution (the universal root) for $D > 0.74$ to multiple solutions (quiescent or turbulent) and eventually to completely turbulent states for $D < 0.08$ (See figure 3). We discovered a slow oscillation of the quiescent reference states corresponding to transitions between bistable states.

In the presence of turbulence, the curve representing the total electromagnetic force, $F_y(\omega)$, changes qualitatively. In particular, the universal root slows down dramatically and loses its universality property (that is, it becomes dependent on the parameters). When the island frequency is allowed to evolve in response to the azimuthal force, a transition to slower states occurs spontaneously. We have observed this transition for different island widths and different kinds of turbulence (drift wave or interchange driven). It thus appears to be a generic phenomenon. The transition always leads to a slower rotation frequency, but its effect on the *magnetic* stability of the tearing perturbation as well as the survival of the turbulence in the final state depends on the width of the island investigated. Indeed, we identify a critical island width, $w_{\rm c}$, such that for $w \lesssim w_{\rm c}$ ($w \gtrsim w_{\rm c}$) the turbulence enhances (respectively, heals) the magnetic island. As an example, for the physical parameters studied and $G = 0$ we show in figure 17 the change in $\Delta_{\rm pol}$ caused by the transition (in this case the *magnetic* stabilization threshold is $w_{\rm c} \cong 3.2$).

We sketch here the nonlinear evolution of a magnetic island in the presence of drift-wave turbulence for $D_{\rm odd} < D < D_{\rm evn}$, as predicted by the results presented above. The island emerges from the linear phase rotating with a frequency comparable to the electron diamagnetic frequency [32] and undergoes a turbulence-induced transition that slows down its rotation frequency and *magnetically* destabilizes it. As a consequence, in the initial nonlinear

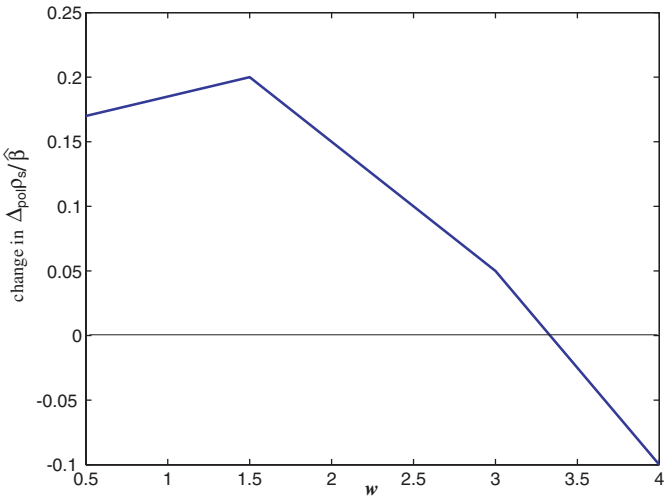

Figure 17. Change in $\Delta_{\rm pol}$ after a turbulence-induced transition versus the imposed island width. The change occurs between the initial state with $u = 1$ and the final state (see figure 13). A positive (negative) value indicates that the transition is magnetically destabilizing (stabilizing).

phase, the island growth is boosted. If the external Δ' is sufficiently large to push the island amplitude beyond $w_{\rm c}$ the turbulence reverses its effect and becomes stabilizing. Finally, if the island keeps growing (due to some other drive), it will quench the turbulence by reducing its drive (the density gradient) inside the separatrix. For smaller values of D, however, the turbulence survives even at large island w.

The introduction of an unfavorable curvature affects the evolution of the magnetic island in two different ways. First, it modifies the quiescent solution by *magnetically* destabilizing the slowly rotating unforced root ($\Delta_{\rm pol}\rho_{\rm s}/\hat{\beta} > 0$). This effect is clearly shown by the parity-enforced reference states. Second, it modifies the nature of the turbulence and increases its strength, thus indirectly affecting the island through the plasma fluctuations. Our results show that also in this case frequency transitions take place. Lastly, we observe that the G-destabilization of the unforced slowly rotating island is reduced by the presence of turbulence.

The results described in this paper have the following two implications for ITER. First, they suggest that turbulence does not dramatically modify the results of the existing theory for the propagation velocity of magnetic island. This diffuses somewhat the most important uncertainty affecting the use of the polarization model to predict the threshold for the NTM. Second, our results show that turbulence *does* play an important role for 'bound' magnetic islands generated by external resonant magnetic perturbations (RMPs), such as those that are used in ELM mitigation strategies. Indeed, we find that turbulence qualitatively modifies the force between the plasma and a bound magnetic island, so that reliable calculations of the edge braking resulting from RMPs requires the consideration of the effects of turbulence.

Acknowledgments

This work was carried out as part of the program of the Center for Multiscale Plasma Dynamics and was supported by the US DOE Contracts No DE-FG03-96ER-54346 and No DE-FC02-04ER54785. The authors acknowledge fruitful discussions with B Breizman and M Ottaviani.

FM is also grateful to L Chacon for his help with the numerical techniques and to G Delzanno and J Finn for stimulating discussions.

References

[1] Rutherford P H 1973 *Phys. Fluids* **16** 1903
[2] Biskamp D 2000 *Magnetic Reconnection in Plasmas* (Cambridge: Cambridge University Press)
[3] La Haye R *et al* 2006 *Phys. Plasmas* **13**
[4] Horton W 1999 *Rev. Mod. Phys.* **71** 735
[5] Inagaki S *et al* 2004 *Phys. Rev. Lett.* **92** 055002
[6] Meiss J D, Hazeltine R D, Diamond P H and Mahajan S M 1982 *Phys. Fluids* **25** 815
[7] Furuya A, Itoh S I and Yagi M 2001 *J. Phys. Soc. Japan* **70** 407
[8] McDevitt C J and Diamond P H 2006 *Phys. Plasmas* **13** 032302
[9] Ishizawa A and Nakajima N 2007 *Phys. Plasmas* **14** 040702
[10] Itoh S-I, Itoh K and Yagi M 2004 *Plasma Phys. Control. Fusion* **46** 123–43
[11] Militello F, Waelbroeck F L, Fitzpatrick R and Horton W 2008 *Phys. Plasmas* **15** 050701
[12] Waelbroeck F L, Connor J W and Wilson H R 2001 *Phys. Rev. Lett.* **87** 215003
[13] Furth H P, Killeen J and Rosenbluth M N 1963 *Phys. Fluids* **6** 459
[14] Hazeltine R D, Kotschenreuther M and Morrison P J 1985 *Phys. Fluids* **28** 2466
[15] Hasegawa A and Wakatani M 1983 *Phys. Rev. Lett.* **50** 682
[16] Scott B D, Biglari H, Terry P W and Diamond P H 1991 *Phys. Fluids* B **3** 51
[17] Hasegawa A and Mima K 1977 *Phys. Rev. Lett.* **39** 205
[18] Waelbroeck F L 2005 *Phys. Rev. Lett.* **95** 35002
[19] Ottaviani M, Porcelli F and Grasso D 2004 *Phys. Rev. Lett.* **93** 075001
[20] Fitzpatrick R, Waelbroeck F L and Militello F 2006 *Phys. Plasmas* **13** 122507
[21] Waelbroeck F L 2007 *Plasma Phys. Control. Fusion* **49** 905
[22] Guzdar P N and Chen L, Kaw P K and Oberman C 1978 *Phys. Rev. Lett.* **40** 1566
[23] Wakatani M, Watanabe K, Sugama H and Hasegawa A 1992 *Phys. Fluids* B **4** 1755
[24] Fitzpatrick R, Watson P G and Waelbroeck F L 2005 *Phys. Plasmas* **12** 082512
[25] Connor J W, Waelbroeck F L and Wilson H R 2001 *Phys. Plasmas* **8** 2835
[26] Scott B D, Hassam A B and Drake J F 1985 *Phys. Fluids* **28** 275
[27] Yu C and Brower D 1992 *Nucl. Fusion* **32** 1545
[28] Fitzpatrick R and Waelbroeck F 2005 *Phys. Plasmas* **12** 122511
[29] Fitzpatrick R and Waelbroeck F 2008 *Phys. Plasmas* **15** 012502
[30] Dorland W and Hammett G 1993 *Phys. Fluids* B **5** 912
[31] Lin Z *et al* 1998 *Science* **281** 1835
[32] Ara G *et al* 1978 *Ann. Phys.* **112** 443